Atmospheric Environment 77 (2013) 781–789

Contents lists available at SciVerse ScienceDirect

Atmospheric Environment

journal homepage: www.elsevier.com/locate/atmosenv

# Effect of mineral dust on secondary organic aerosol yield and aerosol size in $\alpha$-pinene/$NO_x$ photo-oxidation

Chang Liu [a,c], Biwu Chu [b], Yongchun Liu [a,*], Qingxin Ma [a], Jinzhu Ma [a], Hong He [a,**], Junhua Li [b], Jiming Hao [b]

[a] Research Center for Eco-Environmental Sciences, Chinese Academy of Sciences, Beijing 100085, China
[b] School of Environment, Tsinghua University, Beijing 100084, China
[c] Chinese Academy of Meteorological Sciences, Beijing 100081, China

## HIGHLIGHTS

- Alumina seeds lead to a slight reduction in SOA yield due to $O_3$ decomposition.
- Suspended aerosol size depends on mass loading of alumina seeds.
- Condensation of SVOCs onto seeds with low concentration leads to aerosol size growth.
- Dispersion of SVOCs by seeds with high concentration results in aerosol size decrease.

## ARTICLE INFO

*Article history:*
Received 26 February 2013
Received in revised form
8 May 2013
Accepted 27 May 2013

*Keywords:*
Mineral dust
$\alpha$-Pinene
Secondary organic aerosol
Aerosol size
Photo-oxidation

## ABSTRACT

Although it is a significant contributor to atmospheric particles, the role of mineral dust in secondary organic aerosol (SOA) formation has not been fully recognized. In this study, alumina was chosen as the surrogate to investigate the effect of mineral dust on $\alpha$-pinene/$NO_x$ photo-oxidation in a 2 $m^3$ smog chamber at 30 °C and 50% relative humidity (RH). Results showed that alumina seeds could influence both the SOA yield and the aerosol size in the photo-oxidation process. Compared to the seed-free system, the presence of alumina seeds resulted in a slight reduction of SOA yield, and also influenced the final concentration of $O_3$ in the chamber. As an important oxidant of $\alpha$-pinene, the decrease in $O_3$ concentration could reduce the formation of semi-volatile compounds (SVOCs) and consequently inhibited SOA formation. In addition, the size of aerosol was closely related with the mass loading of alumina seeds. At low alumina concentration, SVOCs condensed onto the pre-existing seed surface and led to aerosol size growth. When alumina concentration exceeded about 5 μg $m^{-3}$, SVOC species that condensed to each seed particle were dispersed by alumina seeds, resulting in the decrease in aerosol size.



## 1. Introduction

Particulate matter (PM) is ubiquitous in the atmosphere, and can affect the earth's energy budget or climate by direct effect (scattering and absorbing radiation) and indirect effect (affecting the amounts and physical and radiative properties of clouds through their role as cloud condensation nuclei and/or ice nuclei) (Lohmann and Feichter, 2005; Pilinis et al., 1995). In addition, exposure to aerosol particles, especially fine PM, is associated with adverse effects on human respiratory and cardiovascular systems (Davidson et al., 2005). Organic aerosols make up a substantial fraction of atmospheric fine particles, accounting for 20–90% of aerosol mass in the lower troposphere (Kanakidou et al., 2005). Secondary organic aerosols (SOA) are the dominant fraction of total organic particulate mass (Hallquist et al., 2009). They are produced through the oxidation of volatile organic compounds (VOCs) followed by the gas-particle partitioning of semi-volatile products (Hallquist et al., 2009), or produced by the compounds evaporated from the semi-volatile organic aerosols (Robinson et al., 2007). The chemical and partitioning processes involved depend on a variety of atmospheric conditions, such as hydrocarbon to nitrogen oxide ratios (Cava et al., 2007), temperature (Takekawa et al., 2003), and humidity (Zhou et al., 2011). Inorganic seed particles also play an important role in SOA formation. Previous studies have demonstrated that

* Corresponding author. Tel.: +86 10 62849121.
** Corresponding author. Tel.: +86 10 62849123; fax: +86 10 62923563.
*E-mail addresses:* ycliu@rcees.ac.cn (Y. Liu), honghe@rcees.ac.cn (H. He).

1352-2310/$ – see front matter © 2013 Elsevier Ltd. All rights reserved.
http://dx.doi.org/10.1016/j.atmosenv.2013.05.064

acidic seed particles (such as $(NH_4)_2SO_4$ and $H_2SO_4$) have a catalysis effect on heterogeneous reactions and thus enhance SOA formation (Cao and Jang, 2010; Jang et al., 2002).

Among the atmospheric particles that originate from natural sources, mineral dust (mostly from deserts) is the second largest contributor (1600 Tg $y^{-1}$) to global mass fluxes (Gieré and Querol, 2010). Laboratory studies have revealed that heterogeneous reactions of inorganic trace gases in the atmosphere (e.g. $O_3$, $NO_x$, and $SO_2$) can occur on the surface of mineral dust (Liu et al., 2012; Ma et al., 2008; Usher et al., 2003a). These reactions have a significant effect on the geochemical cycles of trace gas pollutants and the physicochemical properties of atmospheric particles. It has also been found that organic compounds are able to partition onto mineral dust (Liu et al., 2010b; Ma et al., 2010). The loss of atmospheric organic acids due to reactive uptake onto mineral dust particles may be competitive with homogeneous loss pathways, especially in dusty urban and desertified environments (Tong et al., 2010). In addition, methacrolein (MAC) and methyl vinyl ketone (MVK) are irreversibly adsorbed on $\alpha$-$Al_2O_3$ and can rapidly react on the surfaces to form various products such as aldehydes, organic acids, and even high molecular weight compounds (Zhao et al., 2010). Even for volatile organic compounds (acetic acid, formaldehyde, and methanol), the comparable reaction rates between heterogeneous (on $\alpha$-$Fe_2O_3$, $\alpha$-$Al_2O_3$, and $SiO_2$ surfaces) and homogeneous reactions suggest that heterogeneous reactions on mineral dust are competitive with gas-phase chemical reactions (Carlos-Cuellar et al., 2003). These studies suggest that mineral dust may have influence on SOA formation. At present, however, the effect of mineral dust on SOA formation remains unknown.

In this study, photochemical reactions of $\alpha$-pinene/$NO_x$ systems were investigated in an indoor smog chamber. Suspended alumina, which is usually used as the model oxide for mineral dust in laboratory studies, was chosen as the seeds. The influence of mineral seeds on SOA yield and aerosol size was discussed.

## 2. Experimental section

Detailed descriptions of the smog chamber and the instrumentations have been given previously (Chu et al., 2012; Lu et al., 2009). Briefly, a cuboid reactor, with a volume of 2 $m^3$ and a surface-to-volume ratio of 5 $m^{-1}$, was constructed from 50 μm-thick FEP-Teflon film. The temperature of the chamber was precisely controlled at 30 ± 0.5 °C. Prior to each experiment, the chamber was flushed continuously for 40 h with purified compressed air and then exposed to UV light for 20 h. Finally, humid air was introduced into the chamber to obtain a specific relative humidity (RH) of 50%. Temperature, UV radiation, and RH were monitored continuously during the experiments.

Alumina seeds were produced via a spray pyrolysis setup (Liu et al., 2010a). In all experiments, liquid alumisol (AlOOH, Lot No. 2205, Kawaken Fine Chemicals Co., Ltd.), used as the precursor, was sprayed to droplets by an atomizer and dried by a diffusion dryer. The particles were then carried into the corundum tube embedded in the tubular furnace with the temperature maintained at 1000 °C. Finally, the generated alumina particles were introduced into the chamber through a neutralizer. The obtained particles were spherical-shaped $\gamma$-$Al_2O_3$ with the main particle size at about 160 nm (Liu et al., 2010a). Particle size distribution of alumina seeds is shown in Fig. 1. After the introduction of alumina seeds, $\alpha$-pinene (Analytical reagent, Sigma Aldrich Fluka) was injected by syringe into a heated furnace and then carried into the chamber by 5 L $min^{-1}$ purified air. Finally, NO and $NO_2$ were introduced and the photochemical reaction was initiated by turning on 40 blacklights (GE F40BLB, 40 W, 300–400 nm). The gases used in this experiment are summarized in Table 1, and the detailed instruments are listed in Table 2. Total aerosol mass concentration was determined from the observed total aerosol volume by a scanning mobility particle sizer (SMPS, TSI 3936) consisting of a nano differential mobility analyzer (DMA, TSI 3085) and a condensation particles counter (CPC, TSI 3025A). The formed aerosol particles were assumed to be geometrically spherical, and the density was considered to be 1.3 g $cm^{-3}$ according to previous studies (Davidson et al., 2005; Ng et al., 2007). Count median diameter (CMD) determined by SMPS was used to express the average particle size of aerosols.

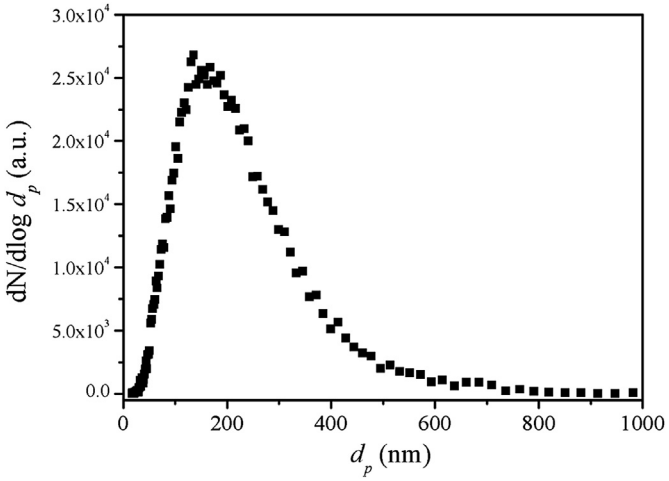


**Fig. 1.** Particle size distribution of 20.5 μg $m^{-3}$ alumina seeds.

Using the smog chamber, a series of experiments were carried out for $\alpha$-pinene photo-oxidation in the presence of $NO_x$. Experimental conditions and results were listed in Table 3. The "Experiment No." were designed to [initial concentration of $\alpha$-pinene] Pin – [initial concentration of $Al_2O_3$]Al. For example, "150Pin-0Al" represents experiment with initial conditions of 150 ppb $\alpha$-pinene and 0 μg $m^{-3}$ $Al_2O_3$. The initial $\alpha$-pinene concentration levels were kept at 150, 200, 250, or 300 ppb. The initial molar ration of $\alpha$-pinene to $NO_x$ was fixed at 2. All experiments were conducted at a temperature of 30 ± 0.5 °C and 50% RH with irradiation of UV light. Experimental duration was set to 4 h.

## 3. Results and discussion

### 3.1. Calculation of SOA yields

#### 3.1.1. Correction of wall loss

Due to the deposition of particles onto the Teflon film, the measured aerosol concentration has to be corrected in each experiment. The rate of particle deposition is proportional to the particle concentration and depends on particle size, leading to first-order kinetics (Cocker III et al., 2001; Carter et al., 2005):

$$\frac{dN(d_p,t)}{dt} = -k_{dep}(d_p)\cdot N(d_p,t) \quad (1)$$

**Table 1**
Summary of gases used in the chamber experiments.

| Gas | Purity | Balance gas | Purpose | Commercial sources |
|---|---|---|---|---|
| NO | 200 ppm | $N_2$ | Reactive gas | AP Beifen Gases Ind. |
| $NO_2$ | 198 ppm | $N_2$ | Reactive gas | AP Beifen Gases Ind. |
| $\alpha$-Pinene | 0.501 ppm | $N_2$ | Standard gas for GC | Takachiho Chemical Industrial Co., LTD. |
| He | ≥99.999% | $N_2$ | Carrier gas for GC | AP Beifen Gases Ind. |

**Table 2**
Summary of instruments used in the chamber experiments.

| | Instrument | Measurement interval (min) | Accuracy |
|---|---|---|---|
| VOCs | Beifen SP-3420 | 15 | 10 ppb |
| $NO_x$ | TEI Model 42C | 1 | 0.4 ppb |
| $O_3$ | TEI Model 49C | 1 | 1.0 ppb |
| Aerosol particles | TSI SMPS 3936 | 6 | – |
| $T$ and RH[a] | Vaisala HMT 333 | 1 | 0.1 °C, 0.5% RH |
| UV | Handy UV-A | 1 | 0.5% |

[a] $T$: temperature; RH: relative humidity.

where $k_{dep}$ ($h^{-1}$) is the deposition rate constant, $N$ (particles $cm^{-3}$) is the number concentration of aerosols, and $d_p$ (nm) is the aerosol diameter. The value of $k_{dep}$ depends on diameter $d_p$ and can be expressed as follows (Takekawa et al., 2003; Takekawa, 2003):

$$k_{dep}(d_p) = a \times d_p^b + c/d_p^d \quad (2)$$

The resulting $k_{dep}$ values for different $d_p$ (20–1000 nm) were determined by monitoring the particle number decay under dark conditions at low initial concentrations (<1000 particles $cm^{-3}$) to avoid serious coagulation. Based on more than 500 sets of $k_{dep}$ values, the optimized values of parameter a–d were calculated to be $6.4579 \times 10^{-7}$, 1.7841, 13.1947, and −0.9566, respectively (Chu et al., 2012). In our previous work, the wall loss was accounted for an average of approximately 4% of total SOA mass from α-pinene photo-oxidation (Chu et al., 2012).

### 3.1.2. SOA yield calculation

The fractional aerosol yield ($Y$) is widely used as an empirical expression to represent the aerosol formation potential of the hydrocarbon (Pandis et al., 1992). It is defined as the ratio of generated organic aerosol concentration $M_o$ (μg $m^{-3}$) to the reacted hydrocarbon concentration $\Delta HC$ (μg $m^{-3}$):

$$Y = \frac{M_o}{\Delta HC} \quad (3)$$

In this work, concentrations of produced aerosol ($M_o$) and reacted α-pinene ($\Delta Pin$) obtained at the end of the experiments were used to calculate the overall aerosol yield ($Y$). Experimental results are summarized in Table 3. Concentrations of generated aerosol $M_o$ contained both suspended and deposited aerosol concentration.

Odum et al. (1996) developed a gas-particle absorptive partitioning model to describe the phenomenon that $Y$ largely depends on the amount of organic aerosol mass concentration:

$$Y = M_o \sum_i \frac{\alpha_i K_{om,i}}{1 + K_{om,i} M_o} \quad (4)$$

where $\alpha_i$ is the mass-based stoichiometric coefficient for the reaction generating product $i$, and $K_{om,i}$ ($m^3$ $\mu g^{-1}$) is the gas-particle partition constant. Eq. (4) can be simplified to one-product ($i = 1$) or two-product ($i = 2$) models by assuming that all semi-volatile products are classified into one or two groups. Although the latter is usually used for fitting yield data (Odum et al., 1996, 1997), the one-product model is of sufficient accuracy to describe the relationship between aerosol yield and mass (Henry et al., 2008; Takekawa et al., 2003; Verheggen et al., 2007). Therefore, one-product model was adopted to fit the experimental yield data versus $M_o$ with a least square method. Yield curve of the experiments and parameters of $\alpha_i$ and $K_{om,i}$ were obtained via the fitting procedure.

## 3.2. Effect of alumina seeds on SOA yield

### 3.2.1. SOA yield results

The results of α-pinene/$NO_x$ photo-oxidation experiments at 30 °C, 50% RH with irradiation of UV light are listed in Table 3. Fig. 2 illustrates SOA yield against the concentration of organic aerosols produced from α-pinene photo-oxidation. As seen from Fig. 2, the yield curve of the experiments with alumina seeds was slightly lower than that of the seed-free experiments. Up and low 95% confidence level lines (dot lines in Fig. 2) also indicated that SOA curve obtained in seed-free experiments was beyond the confidence interval of the seeded experiments data. It implies that the presence of alumina seeds could inhibit the SOA yields in α-pinene/$NO_x$ photo-oxidation, although the inhibition effect is not great.

### 3.2.2. Analysis on the inhibition effect

Secondary organic aerosols are formed via VOC reactions with gaseous oxidants (e.g. $O_3$, OH, $NO_3$) to generate semi-volatile and nonvolatile products (Kroll and Seinfeld, 2008). The formed semi-

**Table 3**
Summary of smog chamber experiments.[a]

| Experiment no. | $[Pin]_0$ (ppb) | $[Al_2O_3]_0$ (μg $m^{-3}$) | $[NO]_0$ (ppb) | $[NO_2]_0$ (ppb) | $[Pin]_0/[NO_x]_0$ (ppb $ppb^{-1}$) | $M_o$ (μg $m^{-3}$) | ΔPin (ppb) | $Y$ (%) |
|---|---|---|---|---|---|---|---|---|
| 150Pin-0Al | 156 | 0 | 38.60 | 37.41 | 2.05 | 33.826 | 150.2 | 4.108 |
| 150Pin-4Al | 159 | 4.0 | 37.30 | 39.80 | 2.06 | 65.104 | 159.2 | 7.462 |
| 150Pin-51Al | 146 | 51.2 | 40.30 | 37.74 | 1.87 | 40.287 | 145.7 | 5.044 |
| 200Pin-0Al | 217 | 0 | 47.28 | 50.53 | 2.21 | 92.443 | 202.5 | 8.333 |
| 200Pin-4Al | 214 | 3.9 | 55.65 | 55.43 | 1.93 | 65.26 | 213.4 | 5.577 |
| 200Pin-20Al | 205 | 20.5 | 50.40 | 44.87 | 2.15 | 66.911 | 204.3 | 5.980 |
| 200Pin-35Al | 216 | 34.9 | 53.25 | 49.62 | 2.09 | 76.648 | 215.0 | 6.500 |
| 200Pin-52Al | 209 | 51.8 | 53.84 | 49.24 | 2.02 | 73.905 | 209.0 | 6.448 |
| 250Pin-0Al | 259 | 0 | 64.54 | 67.47 | 1.96 | 122.707 | 258.3 | 8.671 |
| 250Pin-5Al | 243 | 5.5 | 56.45 | 65.37 | 1.99 | 110.357 | 242.4 | 8.307 |
| 250Pin-20Al | 246 | 19.8 | 55.19 | 67.31 | 2.00 | 88.790 | 245.0 | 6.617 |
| 250Pin-35Al | 294 | 34.7 | 60.12 | 69.86 | 2.26 | 91.130 | 293.6 | 5.668 |
| 250Pin-43Al | 247 | 42.5 | 55.39 | 63.95 | 2.06 | 88.543 | 246.7 | 6.552 |
| 300Pin-0Al | 303 | 0 | 74.06 | 81.73 | 1.94 | 202.826 | 311.2 | 11.895 |
| 300Pin-5Al | 292 | 5.4 | 66.15 | 80.52 | 1.99 | 149.149 | 290.7 | 9.360 |
| 300Pin-46Al | 298 | 45.5 | 72.41 | 79.68 | 1.96 | 89.310 | 277.1 | 5.876 |

$[Pin]_0$: initial concentrations of α-pinene; $[Al_2O_3]_0$: initial concentrations of $Al_2O_3$ seeds; $[NO]_0$: initial concentrations of NO; $[NO_2]_0$: initial concentrations of $NO_2$; $[Pin]_0/[NO_x]_0$: initial molar ration of α-pinene to $NO_x$; $M_o$: total organic aerosol mass concentration produced; ΔPin: total concentration of α-pinene consumed; $Y$: overall aerosol yield.

[a] All the experiments were carried out at 30 °C and 50% RH with irradiation of UV light.

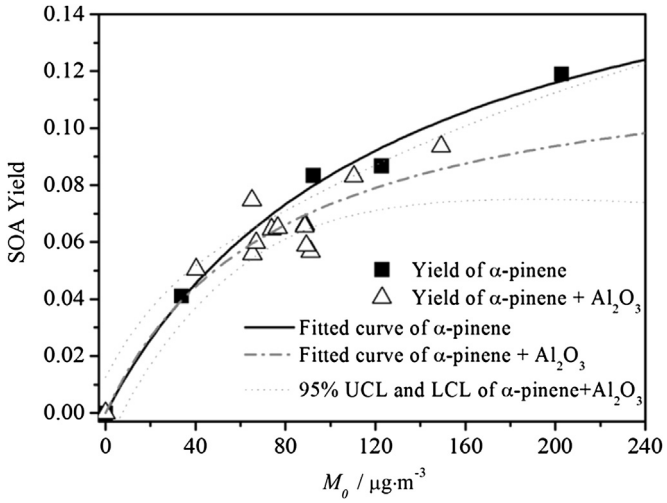


**Fig. 2.** SOA yield ($Y$) as a function of generated organic aerosol mass ($M_o$) for α-pinene photo-oxidation with (△) or without (■) alumina seeds at 30 °C and 50% RH. The dash dot and solid curves are fitted by the one-product model of yields with and without seeds, respectively. UCL: up 95% confidence level; LCL: low 95% confidence level.

volatile and nonvolatile species as well as the compounds evaporated from SVOCs partition to the aerosol phase, resulting in the SOA formation (Hallquist et al., 2009; Robinson et al., 2007). Therefore, the oxidants that initiate the degradation of VOCs are the controlling factor in determining the distribution and volatility of products. Comparison of the new particle formation potential during α-pinene oxidation indicated a drastically higher nucleation potential of the ozonolysis than in the reaction with either OH or $NO_3$ (Bonn and Moortgat, 2002). Model calculation results show that ozonolysis contributes about twice more to SOA formation than oxidation by OH, and thus is confirmed as the most favorable route to aerosol formation (Capouet et al., 2008). Besides, the reaction with $O_3$ represents 46% of the total sink of α-pinene at the global scale; $O_3$ is calculated to be the main oxidant over remote forests (Capouet et al., 2008). In this study, we on-line monitored $O_3$ concentration in the chamber and the dynamic changes of $O_3$ are shown in Fig. 3. Comparing to the seed-free experiments, although the addition of alumina seeds has no influence on the initial formation of $O_3$, the final concentration of $O_3$ is obviously decreased. The decrease of $O_3$ concentration was more obvious in the experiments with high α-pinene concentration. At low α-pinene concentration, the variation of $O_3$ concentration due to the addition of alumina seeds was not obvious, meanwhile the difference of SOA yields between seed-free and seeded experiments was quite subtle (as shown in Fig. 2). Therefore, it is considered that the presence of high concentration alumina seeds might influence the concentration of $O_3$ in the chamber. Moreover, previous research has indicated that during the ozonolysis, the isomerization and decomposition of generated hydroperoxide intermediate species leads to the formation of OH radicals (Di Carlo et al., 2004; Paulson and Orlando, 1996; Zhang et al., 2002; Zhang and Zhang, 2005), and OH aging significantly increases the concentration of first-generation biogenic SOA (Donahue et al., 2012). Besides, photolysis of $O_3$ also contributes to the OH production via the following mechanism (Wine and Nicovich, 2012):

$$O_3 \xrightarrow[h\nu]{300\ \text{nm}<\lambda<340\ \text{nm}} O_2 + O(^1D) \quad (5)$$

$$O(^1D) + H_2O \rightarrow 2OH \quad (6)$$

Therefore, the decrease in $O_3$ concentration might reduce the formation of semi-volatile compounds and even affects the secondary yield of OH.

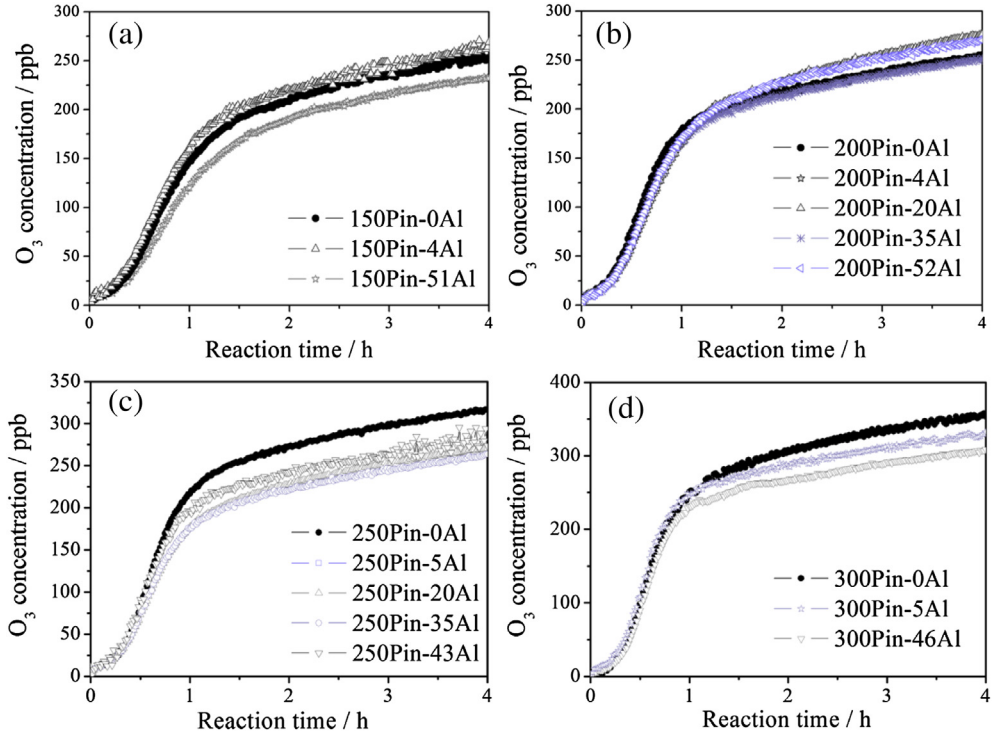


**Fig. 3.** Dynamic change of $O_3$ concentration in (a) 150, (b) 200, (c) 250, and (d) 300 ppb α-pinene photo-oxidation system with different concentration of alumina seeds at 30 °C and 50% RH.

The parameters of $\alpha_i$ and $K_{om,i}$ for the seed-free experiments ($\alpha_{Pin}$, $K_{Pin}$) or seeded experiments ($\alpha_{Pin/Al}$, $K_{Pin/Al}$) in $\alpha$-pinene/$NO_x$ photo-oxidation were determined by the one-product model. The stoichiometric coefficient $\alpha_i$ represents the total amount of the semi-volatile compounds (SVOCs) produced in both gas and aerosol phases, while $K_{om,i}$ is the gas-particle partitioning potential of the semi-volatile compounds produced (Henry et al., 2008). When alumina seeds presented in the system, $\alpha_{Pin}$ decreased from 0.1898 to $\alpha_{Pin/Al}$ of 0.1297. This implied the formation of SVOCs was depressed by the addition of alumina, which was in accordance with the results deduced from the decrease of $O_3$ concentration. Besides $\alpha_i$, $Y$ is also positively correlated to $K_{om,i}$ (as shown by Eq. (4)). In contrast to the change of $\alpha_i$, the value of $K_{Pin}$ increased from 0.00785 to $K_{Pin/Al}$ of 0.01295, implying the saturation vapor pressure of generated SVOC compounds was decreased due to the presence of alumina. The different trends of $\alpha_i$ and $K_{om,i}$ might lead to the fact that the depress on the SOA yield because of alumina seeds was not significant. The variation of $\alpha_i$ and $K_{om,i}$ also suggested that the formation and participation of produced organic species might be influenced by alumina seeds. However, further qualitative and quantitative studies on the gas-phase and aerosol-phase species were not available here due to the lack of instruments, such as proton-transfer reaction mass spectrometry, or single particle mass spectrometry.

Formation of $O_3$ during photo reactions is mainly via the photolysis of $NO_x$. The reaction processes are as follows:

$$2NO + O_2 \rightarrow 2NO_2 \quad (7)$$

$$NO_2 \xrightarrow[h\nu]{285\ nm<\lambda<375\ nm} NO + O(^3P) \quad (8)$$

$$O(^3P) + O_2 \rightarrow O_3 \quad (9)$$

Comparing the $NO_x$ concentration between seed-free experiments and those with alumina seeds, as shown in Fig. 4, the addition of alumina has no influence on the dynamic change of NO and $NO_2$ concentration. This implied that the transformation from NO to $NO_2$ as well as the formation of $O_3$ from the photolysis of $NO_2$ was not disturbed by the presence of alumina. As discovered above, however, alumina seeds indeed decreased the final concentration of $O_3$ in the chamber. We considered this result might be attributed to the adsorption, uptake, and decomposition reaction happened on alumina surface. The reactive uptake coefficients, reaction mechanism, and kinetics of $O_3$ on dust particles have been widely studied previously (El Zein and Bedjanian, 2012; Michel et al., 2003; Roscoe and Abbatt, 2005; Usher et al., 2003a,b). The initial reactive uptake coefficient, $\gamma_{0,BET}$, for alumina powders was measured to be $1.2 \pm 0.4 \times 10^{-4}$ at 296 K using a Knudsen cell apparatus (Michel et al., 2003). The decomposition mechanism for $O_3$ on metal oxides was summarized below (Oyama, 2000; Usher et al., 2003a):

$$O_3 + * \rightarrow O^* + O_2 \quad (10)$$

$$O_3 + O^* \rightarrow O_2^* + O_2 \quad (11)$$

$$O_2^* \rightarrow * + O_2 \quad (12)$$

In this work, we also carried out experiment of $O_3$ decomposition and adsorption on alumina sample. Figure S1 in Supplementary Material clearly illustrated the decomposition of $O_3$ on alumina. Therefore we consider that in the smog chamber the catalytic decomposition of $O_3$ on alumina surface results in the reduction of $O_3$ concentration. Because $O_3$ is an important oxidant of $\alpha$-pinene, a decrease in its concentration will reduce the formation of SVOC products and OH radicals, affects the further oxidation of intermediate species, and finally inhibits SOA formation.

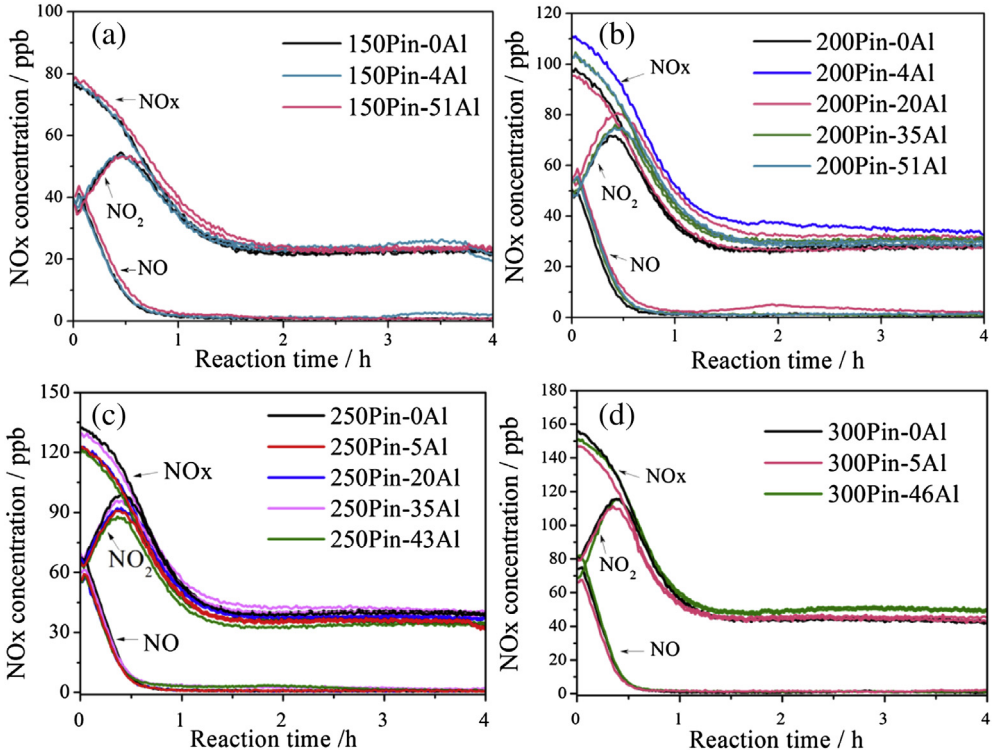


**Fig. 4.** Dynamic change of $NO_x$ concentration in (a) 150, (b) 200, (c) 250, and (d) 300 ppb $\alpha$-pinene photo-oxidation system with different concentration of alumina seeds at 30 °C and 50% RH.

### 3.3. Effect of alumina on aerosol size

#### 3.3.1. Evolution of suspended aerosol size

As an important characteristic of aerosols, particle size directly relates to the light scattering property, cloud condensation nuclei (CCN) potential, and lifetime of aerosols. Therefore, we further investigated the effect of alumina on aerosol size in the α-pinene/$NO_x$ photo-oxidation systems.

200 ppb α-pinene system was taken as the example to illustrate the change of aerosol size distribution during the photo-oxidation. As shown in Fig. 5a, size distribution of suspended aerosol in seed-free experiment (200Pin-0Al) changed obviously with the reaction time. There was no new aerosol particles formation at the beginning of photo-oxidation. Formation of $O_3$ and free radicals dominated the photo reaction and initiated homogeneous nucleation. After the accumulation of SVOC species, (about 45 min later), rapid generation of new aerosols and obvious increase in particle size was observed. The final aerosol size stabilized at about 400 nm after the completion of photo-oxidation.

When 3.9 μg $m^{-3}$ alumina seeds were injected into in the system (Fig. 5b, 200Pin-4Al), formation of new particles was observed after 0.5 h reaction. The generation of aerosols occurred about 15 min earlier than the seed-free experiment, implying that the condensation of SVOCs onto the pre-existing seeds let to the growth of particle size. The diameter of particles increased to 450 nm after 2 h. It should be noted that the final aerosol size was larger than the size obtained in the seed-free experiment.

With the presence of 51.7 μg $m^{-3}$ alumina seeds in the reaction system (Fig. 5c, 200Pin-52Al), the main particle size at the beginning was about 160 nm, which was in accordance with the size distribution of alumina particles. However, the growth of aerosol size was significantly reduced. Aerosol size grew to only about 230 nm after 4 h reaction. The reduction of aerosol size should be unrelated to the deposition of alumina seeds, since the diameter of seed particles remained steady at around 160 nm during the deposition experiments of alumina (Fig. 5d).

As shown above, the size change of aerosols was closely related with the mass loadings of alumina seeds. Therefore, we compared the final size of suspended aerosols formed in the α-pinene/$NO_x$ photo-oxidation system as a function of alumina seeds mass loading. As seen in Fig. 6, the suspended aerosol diameters obtained with low alumina loading (~5 μg $m^{-3}$) were all larger than those obtained in the seed-free experiments. Nevertheless at higher alumina loadings, the size values of aerosols decreased significantly with the increase of alumina concentrations. For instance, in the 300 ppb α-pinene/$NO_x$ system, aerosol size increased from 452 nm to 515 nm due to the introduction of 5.4 μg $m^{-3}$ alumina, whereas decreased to 268 nm when the concentration of alumina was increased to 45.5 μg $m^{-3}$.

In previous studies, the condensation of semi-volatile products onto the surface of pre-existing particles led to aerosol growth. For example, Arizona test dust and illite particles were coated with SOA formed by α-pinene ozonization in a cloud simulation chamber (Möhler et al., 2008). The comparison of number size distributions before and after coating indicated that the condensation of SOA on these mineral particles led to the increase in the number of larger aerosol particles. In the present work, however, the growth of aerosols only presented with low seed concentrations. At higher

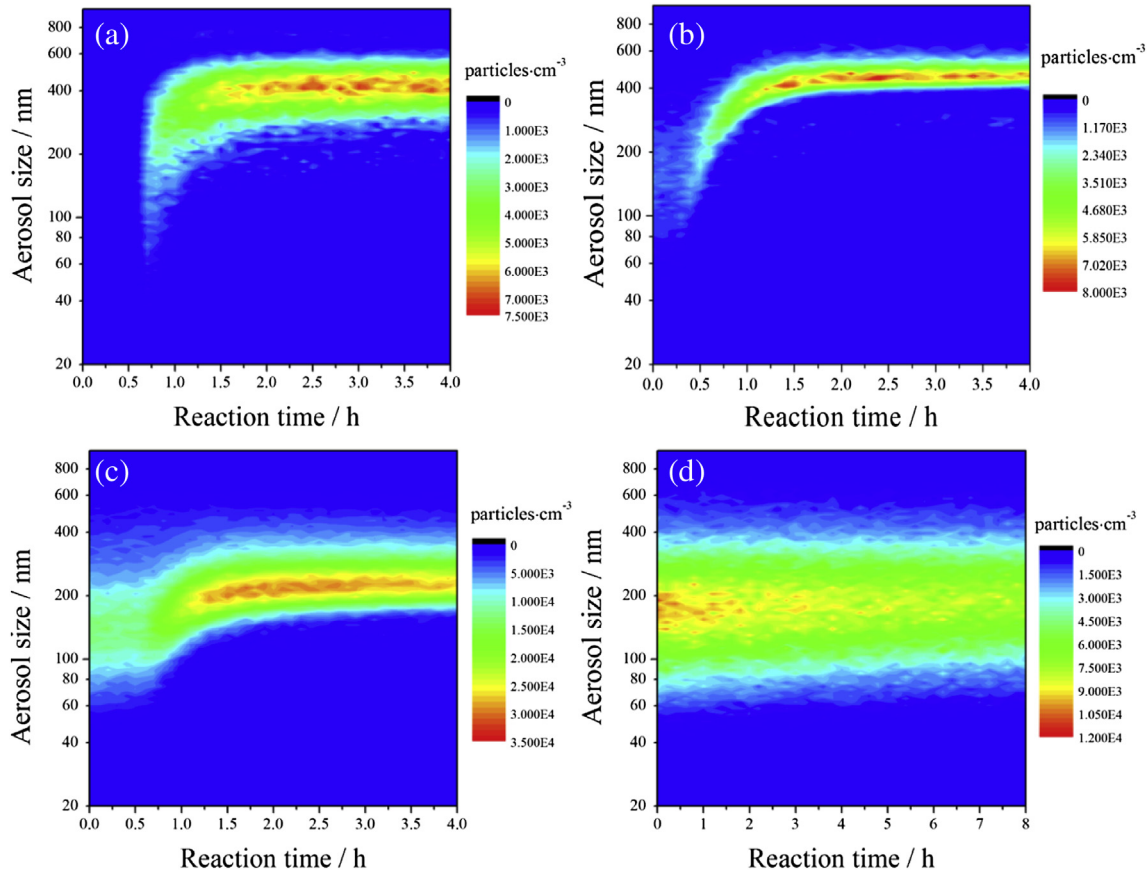


**Fig. 5.** Change of aerosol size distribution and aerosol concentration as a function of time in experiments of (a) 200Pin-0Al, (b) 200Pin-4Al, (c) 200Pin-52Al, and (d) 50Al. Deposition experiments of alumina seeds were conducted at 30 °C and 50% RH for 8 h.

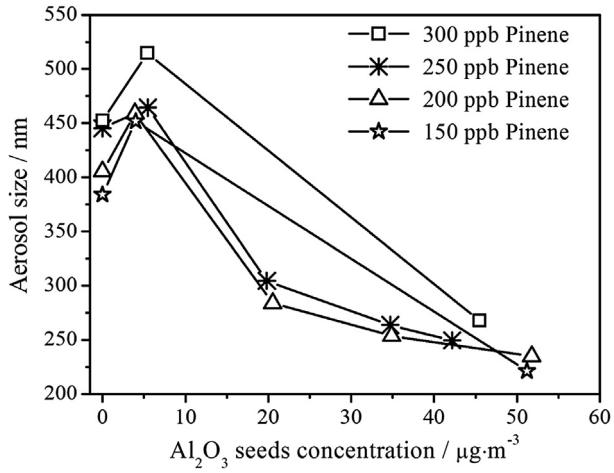


**Fig. 6.** Change of aerosol size as a function of alumina seeds concentration. Aerosol size is described by the final value of count median diameter (CMD) obtained in α-pinene photo-oxidation systems at 30 °C and 50% RH with the reaction time of 4 h. Each data point corresponds to a separate experiment.

concentrations, aerosol size decreased with the increase of alumina concentration.

### 3.3.2. Mechanism proposed for the variation of aerosol size

Mechanism proposed for the seed effect on the aerosol size is shown in Fig. 7. Formation of SOA particles began with the generation of numerous SVOC species forming from the photo-oxidation of α-pinene. After the accumulation of the SVOCs, SOA particles formed via homogeneous or heterogeneous nucleation process. For instance, in the experiment of 300 ppb α-pinene photo-oxidation, homogeneous nucleation of SVOC species resulted in the formation of SOA particles with the size of 452 nm. When alumina seeds of low concentration (5.4 μg $m^{-3}$) presented in the reaction system, SVOC species preferred to coagulate and condense onto the existing seed surface to form SOA particles with a diameter of 515 nm.

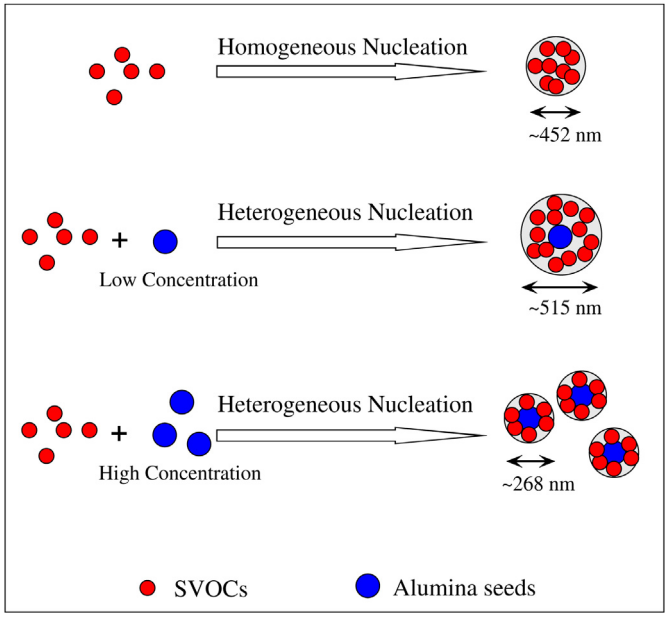


**Fig. 7.** Impact of alumina seeds on SOA diameter. Experiments of 300 ppb α-pinene photo-oxidation were taken as the example to show the diameters of formed SOA particles.

Comparing to the homogenous nucleation, this heterogeneous nucleation process led to an increase in the aerosol size. Considering that the effect of alumina on SOA yield was not significant in α-pinene photo-oxidation, the growth of aerosol particles will result in the decrease of aerosol number concentration. This phenomenon has been demonstrated by the dynamic change of aerosol number concentrations in Figure S2. When high concentration (45.5 μg $m^{-3}$) seeds were introduced into the system, SOA particles also formed via the heterogeneous nucleation process. However, SVOC species were dispersed by these seed particles and the amount of SVOCs that condense to each seed particle was greatly reduced. Therefore, aerosol size decreased obviously to 268 nm. The increase in aerosol number shown in Figure S2 as well as the decrease in aerosol size indicated that SVOCs were dispersed by alumina seeds.

### 3.4. Atmospheric implications

Mineral dust is found to be the largest aerosol component in China, accounting for about 35% of $PM_{10}$ and even reaching from 50% to 60% in northwestern China (Zhang et al., 2012). As an important component of mineral dust, alumina accounts for 10–15% of the dust mass (Usher et al., 2003a). Although the inhibition effect of alumina on SOA yield in α-pinene photo-oxidation is not great, our results at least suggest that the contribution of α-pinene to regional SOA concentration might be influenced by alumina dust. The mass fraction of organic components in sub-micrometer aerosols in Beijing was found to be lower than in other Northern Hemisphere locations (Jimenez et al., 2009). Apart from different emission patterns of pollutants and different meteorological conditions, the lower mass fraction of organic matter may also be partially explained by the restriction effect of the high dust loading in this region. Of course, to fully understand the role of mineral dust in SOA formation, it is necessary to further investigate the effect of other mineral components, such as $SiO_2$ and $Fe_2O_3$, on the SOA formation in the future.

In addition, alumina seeds resulted in aerosol size variation and therefore might have influence on the health effect and light scattering property of aerosols. A reduction in size may enhance the transfer ability of aerosol particles in human respiratory systems (Nel, 2005; Gieré and Querol, 2010). Quasi-ultrafine particles (<180 nm) are more harmful to human health than fine particles (<2.5 μm) (Verma et al., 2011). Accordingly, the decrease in suspended aerosol size due to the presence of alumina dust might result in more serious risks to human health. Furthermore, according to Mie theory, the light scattering property of aerosols changed because of the addition of mineral dust. The details of the Mie scattering calculation as well as the obtained calculations are listed in Table S1 in Supplementary Material. The reduction in the suspended aerosol diameters resulted in a significant decrease in both scattering efficiency and total attenuation coefficient of aerosols. According to Lambert–Beer law, the intensity of transmitted light was therefore increased compared to the seed-free experiment. It means that without the presence of mineral dust, the adverse effect of SOA on atmospheric transparency may be more serious during urban smog episodes.

## 4. Conclusions

Effect of mineral dust on SOA yield and aerosol size in α-pinene/$NO_x$ photo-oxidation was investigated in this work. The SOA yields in α-pinene systems were reduced by the presence of alumina seeds compared to the seed-free system. This inhibition effect might be attributed to the influence of alumina on $O_3$ concentration. Because $O_3$ is critical to both α-pinene oxidation and OH

generation, the decrease in its concentration will reduce the formation of semi-volatile products and even affects the further oxidation of these species, and finally inhibits SOA formation. The presence of seeds also gave rise to the change of aerosol size. At low alumina concentration, SVOCs condensed onto the pre-existing seed surfaces and resulted in aerosol size growth. When alumina concentration was higher than about 5 $\mu g\ m^{-3}$, the decrease in the amount of SVOCs that condensed to each seed particle induced the reduction in the aerosol size.

## Acknowledgments

This research was financially supported by the National Natural Science Foundation of China (20937004), the Strategic Priority Research Program of the Chinese Academy of Sciences (XDB05010300), and the General Financial Grant from the China Postdoctoral Science Foundation (2012M520485).

## Appendix A. Supplementary material

Supplementary material associated with this article can be found, in the online version, at http://dx.doi.org/10.1016/j.atmosenv.2013.05.064.

## References

Bonn, B., Moortgat, G.K., 2002. New particle formation during $\alpha$- and $\beta$-pinene oxidation by $O_3$, OH and $NO_3$, and the influence of water vapour: particle size distribution studies. Atmospheric Chemistry and Physics 2, 183–196.

Cao, G., Jang, M., 2010. An SOA model for toluene oxidation in the presence of inorganic aerosols. Environmental Science & Technology 44, 727–733.

Capouet, M., Müller, J.F., Ceulemans, K., Compernolle, S., Vereecken, L., Peeters, J., 2008. Modeling aerosol formation in alpha-pinene photo-oxidation experiments. Journal of Geophysical Research 113, D02308.

Carlos-Cuellar, S., Li, P., Christensen, A.P., Krueger, B.J., Burrichter, C., Grassian, V.H., 2003. Heterogeneous uptake kinetics of volatile organic compounds on oxide surfaces using a Knudsen cell reactor: adsorption of acetic acid, formaldehyde, and methanol on $\alpha$-$Fe_2O_3$, $\alpha$-$Al_2O_3$, and $SiO_2$. The Journal of Physical Chemistry A 107, 4250–4261.

Carter, W.P.L., Cocker, D.R., Fitz, D.R., Malkina, I.L., Bumiller, K., Sauer, C.G., Pisano, J.T., Bufalino, C., Song, C., 2005. A new environmental chamber for evaluation of gas-phase chemical mechanisms and secondary aerosol formation. Atmospheric Environment 39, 7768–7788.

Cava, S., Tebcherani, S.M., Souza, I.A., Pianaro, S.A., Paskocimas, C.A., Longo, E., Varela, J.A., 2007. Structural characterization of phase transition of $Al_2O_3$ nanopowders obtained by polymeric precursor method. Materials Chemistry and Physics 103, 394–399.

Chu, B.W., Hao, J.M., Takekawa, H., Li, J.H., Wang, K., Jiang, J.K., 2012. The remarkable effect of $FeSO_4$ seed aerosols on secondary organic aerosol formation from photooxidation of $\alpha$-pinene/$NO_x$ and toluene/$NO_x$. Atmospheric Environment 55, 26–34.

Cocker III, D.R., Flagan, R.C., Seinfeld, J.H., 2001. State-of-the-art chamber facility for studying atmospheric aerosol chemistry. Environmental Science & Technology 35, 2594–2601.

Davidson, C.I., Phalen, R.F., Solomon, P.A., 2005. Airborne particulate matter and human health: a review. Aerosol Science and Technology 39, 737–749.

Di Carlo, P., Brune, W.H., Martinez, M., Harder, H., Lesher, R., Ren, X., Thornberry, T., Carroll, M.A., Young, V., Shepson, P.B., Riemer, D., Apel, E., Campbell, C., 2004. Missing OH reactivity in a forest: evidence for unknown reactive biogenic VOCs. Science 304, 722–725.

Donahue, N.M., Henry, K.M., Mentel, T.F., Kiendler-Scharr, A., Spindler, C., Bohn, B., Brauers, T., Dorn, H.P., Fuchs, H., Tillmann, R., Wahner, A., Saathoff, H., Naumann, K., Möhler, O., Leisner, T., Müller, L., Reinnig, M., Hoffmann, T., Salo, K., Hallquist, M., Frosch, M., Bilde, M., Tritscher, T., Barmet, P., Praplan, A.P., DeCarlo, P.F., Dommen, J., Prévôt, A.S.H., Baltensperger, U., 2012. Aging of biogenic secondary organic aerosol via gas-phase OH radical reactions. Proceedings of the National Academy of Sciences of the United States of America 109, 13503–13508.

El Zein, A., Bedjanian, Y., 2012. Interaction of $NO_2$ with $TiO_2$ surface under UV irradiation: measurements of the uptake coefficient. Atmospheric Chemistry and Physics 12, 1013–1020.

Gieré, R., Querol, X., 2010. Solid particulate matter in the atmosphere. Elements 6, 215–222.

Hallquist, M., Wenger, J.C., Baltensperger, U., Rudich, Y., Simpson, D., Claeys, M., Dommen, J., Donahue, N.M., George, C., Goldstein, A.H., Hamilton, J.F., Herrmann, H., Hoffmann, T., Iinuma, Y., Jang, M., Jenkin, M.E., Jimenez, J.L., Kiendler-Scharr, A., Maenhaut, W., McFiggans, G., Mentel, Th.F., Monod, A., Prévôt, A.S.H., Seinfeld, J.H., Surratt, J.D., Szmigielski, R., Wildt, J., 2009. The formation, properties and impact of secondary organic aerosol: current and emerging issues. Atmospheric Chemistry and Physics 9, 5155–5236.

Henry, F., Coeur-Tourneur, C., Ledoux, F., Tomas, A., Menu, D., 2008. Secondary organic aerosol formation from the gas phase reaction of hydroxyl radicals with *m*-, *o*-and *p*-cresol. Atmospheric Environment 42, 3035–3045.

Jang, M., Czoschke, N.M., Lee, S., Kamens, R.M., 2002. Heterogeneous atmospheric aerosol production by acid-catalyzed particle-phase reactions. Science 298, 814–817.

Jimenez, J.L., Canagaratna, M.R., Donahue, N.M., Prévôt, A.S.H., Zhang, Q., Kroll, J.H., DeCarlo, P.F., Allan, J.D., Coe, H., Ng, N.L., Aiken, A.C., Docherty, K.S., Ulbrich, I.M., Grieshop, A.P., Robinson, A.L., Duplissy, J., Smith, J.D., Wilson, K.R., Lanz, V.A., Hueglin, C., Sun, Y.L., Tian, J., Laaksonen, A., Raatikainen, T., Rautiainen, J., Vaattovaara, P., Ehn, M., Kulmala, M., Tomlinson, J.M., Collins, D.R., Cubison, M.J., Dunlea, E.J., Huffman, J.A., Onasch, T.B., Alfarra, M.R., Williams, P.I., Bower, K., Kondo, Y., Schneider, J., Drewnick, F., Borrmann, S., Weimer, S., Demerjian, K., Salcedo, D., Cottrell, L., Griffin, R., Takami, A., Miyoshi, T., Hatakeyama, S., Shimono, A., Sun, J.Y., Zhang, Y.M., Dzepina, K., Kimmel, J.R., Sueper, D., Jayne, J.T., Herndon, S.C., Trimborn, A.M., Williams, L.R., Wood, E.C., Middlebrook, A.M., Kolb, C.E., Baltensperger, U., Worsnop, D.R., 2009. Evolution of organic aerosols in the atmosphere. Science 326, 1525–1529.

Kanakidou, M., Seinfeld, J.H., Pandis, S.N., Barnes, I., Dentener, F.J., Facchini, M.C., Van Dingenen, R., Ervens, B., Nenes, A., Nielsen, C.J., Swietlicki, E., Putaud, J.P., Balkanski, Y., Fuzzi, S., Horth, J., Moortgat, G.K., Winterhalter, R., Myhre, C.E.L., Tsigaridis, K., Vignati, E., Stephanou, E.G., Wilson, J., 2005. Organic aerosol and global climate modelling: a review. Atmospheric Chemistry and Physics 5, 1053–1123.

Kroll, J.H., Seinfeld, J.H., 2008. Chemistry of secondary organic aerosol: formation and evolution of low-volatility organics in the atmosphere. Atmospheric Environment 42, 3593–3624.

Liu, C., Liu, Y.C., Ma, Q.X., He, H., 2010a. Mesoporous transition alumina with uniform pore structure synthesized by alumisol spray pyrolysis. Chemical Engineering Journal 163, 133–142.

Liu, Y.C., Ma, J.Z., Liu, C., He, H., 2010b. Heterogeneous uptake of carbonyl sulfide onto kaolinite within a temperature range of 220–330 K. Journal of Geophysical Research 115, D24311.

Liu, C., Ma, Q.X., Liu, Y.C., Ma, J.Z., He, H., 2012. Synergistic reaction between $SO_2$ and $NO_2$ on mineral oxides: a potential formation pathway of sulfate aerosol. Physical Chemistry Chemical Physics 14, 1668–1676.

Lohmann, U., Feichter, J., 2005. Global indirect aerosol effects: a review. Atmospheric Chemistry and Physics 5, 715–737.

Lu, Z., Hao, J., Takekawa, H., Hu, L., Li, J., 2009. Effect of high concentrations of inorganic seed aerosols on secondary organic aerosol formation in the *m*-xylene/$NO_x$ photooxidation system. Atmospheric Environment 43, 897–904.

Ma, Q.X., Liu, Y.C., He, H., 2008. Synergistic effect between $NO_2$ and $SO_2$ in their adsorption and reaction on $\gamma$-$Al_2O_3$. The Journal of Physical Chemistry A 112, 6630–6635.

Ma, J.Z., Liu, Y.C., He, H., 2010. Degradation kinetics of anthracene by ozone on mineral oxides. Atmospheric Environment 44, 4446–4453.

Michel, A.E., Usher, C.R., Grassian, V.H., 2003. Reactive uptake of ozone on mineral oxides and mineral dusts. Atmospheric Environment 37, 3201–3211.

Möhler, O., Benz, S., Saathoff, H., Schnaiter, M., Wagner, R., Schneider, J., Walter, S., Ebert, V., Wagner, S., 2008. The effect of organic coating on the heterogeneous ice nucleation efficiency of mineral dust aerosols. Environmental Research Letters 3, 025007.

Nel, A., 2005. Air pollution-related illness: effects of particles. Science 308, 804–806.

Ng, N.L., Chhabra, P.S., Chan, A.W.H., Surratt, J.D., Kroll, J.H., Kwan, A.J., McCabe, D.C., Wennberg, P.O., Sorooshian, A., Murphy, S.M., Dalleska, N.F., Flagan, R.C., Seinfeld, J.H., 2007. Effect of $NO_x$ level on secondary organic aerosol (SOA) formation from the photooxidation of terpenes. Atmospheric Chemistry and Physics 7, 10131–10177.

Odum, J.R., Hoffmann, T., Bowman, F., Collins, D., Flagan, R.C., Seinfeld, J.H., 1996. Gas/particle partitioning and secondary organic aerosol yields. Environmental Science & Technology 30, 2580–2585.

Odum, J.R., Jungkamp, T.P.W., Griffin, R.J., Forstner, H.J.L., Flagan, R.C., Seinfeld, J.H., 1997. Aromatics, reformulated gasoline, and atmospheric organic aerosol formation. Environmental Science & Technology 31, 1890–1897.

Oyama, S.T., 2000. Chemical and catalytic properties of ozone. Catalysis Reviews 42, 279–322.

Pandis, S.N., Harley, R.A., Cass, G.R., Seinfeld, J.H., 1992. Secondary organic aerosol formation and transport. Atmospheric Environment 26, 2269–2282.

Paulson, S.E., Orlando, J.J., 1996. The reactions of ozone with alkenes: an important source of $HO_x$ in the boundary layer. Geophysical Research Letters 23, 3727–3730.

Pilinis, C., Pandis, S.N., Seinfeld, J.H., 1995. Sensitivity of direct climate forcing by atmospheric aerosols to aerosol size and composition. Journal of Geophysical Research 100, 18739–18754.

Robinson, A.L., Donahue, N.M., Shrivastava, M.K., Weitkamp, E.A., Sage, A.M., Grieshop, A.P., Lane, T.E., Pierce, J.R., Pandis, S.N., 2007. Rethinking organic aerosols: semivolatile emissions and photochemical aging. Science 315, 1259–1262.

Roscoe, J.M., Abbatt, J.P.D., 2005. Diffuse reflectance FTIR study of the interaction of alumina surfaces with ozone and water vapor. The Journal of Physical Chemistry A 109, 9028–9034.

Takekawa, H., 2003. Secondary organic aerosol formation from photochemical reaction of aromatic hydrocarbons. R&D Review of Toyota CRDL 38, 57–62.
Takekawa, H., Minoura, H., Yamazaki, S., 2003. Temperature dependence of secondary organic aerosol formation by photo-oxidation of hydrocarbons. Atmospheric Environment 37, 3413–3424.
Tong, S.R., Wu, L.Y., Ge, M.F., Wang, W.G., Pu, Z.F., 2010. Heterogeneous chemistry of monocarboxylic acids on $\alpha$-$Al_2O_3$ at different relative humidities. Atmospheric Chemistry and Physics 10, 7561–7574.
Usher, C.R., Michel, A.E., Grassian, V.H., 2003a. Reactions on mineral dust. Chemical Reviews 103, 4883–4940.
Usher, C.R., Michel, A.E., Stec, D., Grassian, V.H., 2003b. Laboratory studies of ozone uptake on processed mineral dust. Atmospheric Environment 37, 5337–5347.
Verheggen, B., Mozurkewich, M., Caffrey, P., Frick, G., Hoppel, W., Sullivan, W., 2007. $\alpha$-Pinene oxidation in the presence of seed aerosol: estimates of nucleation rates, growth rates, and yield. Environmental Science & Technology 41, 6046–6051.
Verma, V., Pakbin, P., Cheung, K.L., Cho, A.K., Schauer, J.J., Shafer, M.M., Kleinman, M.T., Sioutas, C., 2011. Physicochemical and oxidative characteristics of semi-volatile components of quasi-ultrafine particles in an urban atmosphere. Atmospheric Environment 45, 1025–1033.
Wine, P.H., Nicovich, J.M., 2012. Atmospheric radical chemistry. In: Chatgilialoglu, C., Studer, A. (Eds.), Encyclopedia of Radicals in Chemistry, Biology and Materials. John Wiley & Sons, Ltd., New York, pp. 503–528.
Zhang, D., Zhang, R., 2005. Ozonolysis of $\alpha$-pinene and $\beta$-pinene: kinetics and mechanism. The Journal of Chemical Physics 122, 114308.
Zhang, D., Lei, W., Zhang, R., 2002. Mechanism of OH formation from ozonolysis of isoprene: kinetics and product yields. Chemical Physics Letters 358, 171–179.
Zhang, X.Y., Wang, Y.Q., Niu, T., Zhang, X.C., Gong, S.L., Zhang, Y.M., Sun, J.Y., 2012. Atmospheric aerosol compositions in China: spatial/temporal variability, chemical signature, regional haze distribution and comparisons with global aerosols. Atmospheric Chemistry and Physics 12, 779–799.
Zhao, Y., Chen, Z., Zhao, J., 2010. Heterogeneous reactions of methacrolein and methyl vinyl ketone on $\alpha$-$Al_2O_3$ particles. Environmental Science & Technology 44, 2035–2041.
Zhou, Y., Zhang, H., Parikh, H.M., Chen, E.H., Rattanavaraha, W., Rosen, E.P., Wang, W., Kamens, R.M., 2011. Secondary organic aerosol formation from xylenes and mixtures of toluene and xylenes in an atmospheric urban hydrocarbon mixture: water and particle seed effects (II). Atmospheric Environment 45, 3882–3890.